

Review

A Comparative Review of Binder-Containing Extrusion and Alternative Shaping Techniques for Structuring of Zeolites into Different Geometrical Bodies

Zahra Asgar Pour ^{1,*} , Marwan M. Abduljawad ² , Yasser A. Alassmy ² , Ludwig Cardon ³ , Paul H. M. Van Steenberge ⁴  and Khaled O. Sebakhly ^{4,*} 

- ¹ Department of Chemical Engineering, Engineering and Technology Institute Groningen (ENTEG), University of Groningen, Nijenborgh 4, 9747AG Groningen, The Netherlands
 - ² Refining and Petrochemicals Technologies Institute, Center of Excellence for Petrochemicals (Oxford), King Abdulaziz City for Science and Technology (KACST), Riyadh 11442, Saudi Arabia
 - ³ Centre for Polymer and Material Technologies (CPMT), Department of Materials, Textiles and Chemical Engineering, Ghent University, Technologiepark 130 (zone c3), 9052 Ghent, Belgium
 - ⁴ Centre for Polymer and Material Technologies (CPMT), Laboratory for Chemical Technology (LCT), Department of Materials, Textiles and Chemical Engineering, Ghent University, Technologiepark 125, 9052 Ghent, Belgium
- * Correspondence: z.asgar.pour@rug.nl (Z.A.P.); khaled.sebakhly@ugent.be (K.O.S.); Tel.: +31-(0)6-2992-8542 (K.O.S.)



Citation: Asgar Pour, Z.; Abduljawad, M.M.; Alassmy, Y.A.; Cardon, L.; Van Steenberge, P.H.M.; Sebakhly, K.O. A Comparative Review of Binder-Containing Extrusion and Alternative Shaping Techniques for Structuring of Zeolites into Different Geometrical Bodies. *Catalysts* **2023**, *13*, 656. <https://doi.org/10.3390/catal13040656>

Academic Editors: Maja Milojević Rakić and Danica Bajuk-Bogdanović

Received: 26 December 2022

Revised: 29 January 2023

Accepted: 23 March 2023

Published: 27 March 2023



Copyright: © 2023 by the authors. Licensee MDPI, Basel, Switzerland. This article is an open access article distributed under the terms and conditions of the Creative Commons Attribution (CC BY) license (<https://creativecommons.org/licenses/by/4.0/>).

Abstract: Zeolites are crystalline metallosilicates displaying unique physicochemical properties with widespread applications in catalysis, adsorption, and separation. They are generally obtained by a multi-step process that starts with primary mixture aging, followed by hydrothermal crystallization, washing, drying, and, finally, a calcination step. However, the zeolites obtained are in the powder form and because of generating a pressure drop in industrial fixed bed reactors, not applicable for industrial purposes. To overcome such drawbacks, zeolites are shaped into appropriate geometries and desired size (a few centimeters) using extrusion, where zeolite powders are mixed with binders (e.g., mineral clays or inorganic oxides). The presence of binders provides good mechanical strength against crushing in shaped zeolites, but binders may have adverse impacts on zeolite catalytic and sorption properties, such as active site dilution and pore blockage. The latter is more pronounced when the binder has a smaller particle size, which makes the zeolite internal active sites mainly inaccessible. In addition to the shaping requirements, a hierarchical structure with different levels of porosity (micro-, meso-, and macropores) and an interconnected network are essential to decrease the diffusion limitation inside the zeolite micropores as well as to increase the mass transfer because of the presence of larger auxiliary pores. Thus, the generation of hierarchical structure and its preservation during the shaping step is of great importance. The aim of this review is to provide a comprehensive survey and detailed overview on the binder-containing extrusion technique compared to alternative shaping technologies with improved mass transfer properties. An emphasis is allocated to those techniques that have been less discussed in detail in the literature.

Keywords: zeolites shaping technology; binder-containing extrusion; zeolitic monoliths; binder effects; binder-free shaping alternatives; extrusion

1. Introduction

In recent decades, rapidly growing rates in chemical demands from the market and the need for greener considerations for chemical production have accelerated the production and utilization of heterogeneous catalysts and adsorbents in industry. Large-scale application is always dictated by several pre-requisites that have to be fulfilled in order to make these materials suitable for commercial application. Among these requirements, shaping is one of the most important steps, since bulk zeolites in powder form will increase

the pressure drop in packed bed reactors [1,2]. Conversely, shaped bodies with larger particle sizes (several mm) and a high degree of mechanical resistance to abrasion and dust formation are appropriate to minimize the pressure drop in a fixed-bed setup [3], and, thus, are good candidates for high throughput processes as well. Each shaped catalyst displays a specific flow pattern, which is more influenced by flow direction (e.g., up- or down-flow mode) [4], while a powder-loaded bed is a compact structure where the lack of enough void space complicates reactant feed in, permeability, and well-mixing across the bed, and, consequently, impedes the establishment of a steady-state flow regime inside the bed. Furthermore, powder application increases the volume of the bed for a given reactant flow rate, which, in turn, gives rise to the fabrication costs as well.

Zeolites as crystalline metallosilicates, conventionally in the form of aluminosilicates, have well-defined microporous networks containing regular cavities and channels [5]. Up to now, various excellent features have been reported for zeolites, such as molecular sieving, shape selectivity, high surface area, pore size tuning, high thermal and hydrothermal stability, tunable acidity, crystallinity, and ion-exchange property [6–12]. However, despite the outstanding features exhibited by zeolites, they are inherently microporous materials ($d_{\text{pore}} < 1.5$ nm) and, thus, suffer from intense diffusion limitations imposed by their micropores, particularly, in contact with bulky molecules [12]. In brief, molecules larger than the diameter of micropores are not able to diffuse through the narrow openings of pores and, thus, have a low chance of accessing the zeolite internal active sites. To overcome the microporosity limitations, many strategies such as synthesis of nano-size zeolites, structuring large pore size zeolites, and the design of hierarchical zeolite have been exploited to enhance the molecular diffusion [13–15]. For the sake of clarity, nano-size zeolites can diminish the diffusion limitations drawback of conventional micron-size zeolites due to their larger external surface area, which can be utilized for molecular adsorption and catalysis of bulkier species which cannot diffuse into the micropores. In addition, reduced mean diffusion path in nano-size zeolites can enhance the molecular diffusion rate by means of the shorter path length.

In addition, application of zeolite in industrial scale is strongly interrelated to the shaping technologies applied for structuring zeolite powder, where their fundamental microscopic physico-chemical properties (e.g., acidity, porosity, surface area) are highly dependent on the engineering features of macroscopic catalytic bodies (e.g., transport phenomena and pressure drop in packed bed reactors). Moreover, the utmost preservation of intrinsic catalytic properties is imperative during the shaping step, which provides adequate mechanical strength to the shaped bodies. Thanks to their resistance against breakage or abrasion as well as preventing high pressure drops, structured bodies are applicable for large scale operation conditions (e.g., high pressures and temperatures). Structuring is possible into final bodies with several different geometries (e.g., pellets, cylinders, honeycomb monoliths, hollow alternatives, etc.) [16,17]. Basically, the type of reactor dictates what geometry is more suitable. For instance, large shaped bodies are suitable for packed and moving beds, which are mainly prepared using extrusion, pelletizing, or granulation (with approximate pellet size in the range of 1 mm up to 3 cm). However, for slurry three phase reactors and fluidized beds, powders with a particle size in the range of 20 to 100 μm (prepared via spray drying) are more applicable [18]. In the subject of shaping, some researchers have tested lab-made zeolite bodies in larger pilot equipment [19–21], but less focus has been methodically directed toward shaping techniques their pros and cons, and their effects on the zeolite physicochemical properties. On the basis of what we have found so far, macroscopic shaping technologies of zeolites have been never completely collected and discussed in one study in detail. This motivated us to prepare this review from academic research and industrial patents, with the impetus of elucidation of the influence of several shaping methods, such as binder-containing extrusion technique and binder-free alternatives on the physico-chemical properties and performance of zeolites bodies. Moreover, the future outlook is depicted for more practical shaping techniques.

2. Zeolites Shaping Using Extrusion Technique and by Means of Inorganic and/or Organic Binders

The extrusion technique is frequently carried out in industry to shape powders with various geometries (e.g., cylinders, hollow cylinders, monoliths, etc.) to form extrudates with an average length range of 0.5–2 cm [22–24]. A schematic illustration of the extrusion process and some examples of commercial extrudates are shown in Figure 1A,B, respectively. Generally, there are some parameters that need to be smartly tuned to provide sufficient pastiness and rheological integrity, such as water mass ratio [25], which is determined on the basis of empirical trials, mixing and aging times [18], and binder content [26,27] as well as drying and calcination temperature. The mechanical strength of extrudates is mainly obtained by the adhesive interaction and partial interconnection of zeolite terminal hydroxyl groups with the adjacent binder particles, or by a fusion between contacting surfaces of binder and zeolites particles that is more pronounced after the calcination step [28]. The applied quantities of binders are varied and even values higher than 50 wt% were reported [29], but the more preferable amounts of binders are in the range of 10 to 20 wt% [29]. Binders not only provide good mechanical stability to zeolites but also some types of binders, such as oxides (e.g., alumina), improve the activity of silicate materials with low or no acidity [30]. The type of binder is normally selected on the basis of shaping necessities and the relevant application requirements [25]. In general, two types of common binders are used for zeolite shaping: inorganic binders (e.g., clays, silica, alumina, titania, zirconia, or a combination of them) and organic binders (e.g., water-soluble cellulose products, polyethylene glycol, and polyvinyl alcohol.) [31]. Organic binders are more applicable as thickening additives, lubricants, wetting agents, and plasticizers [26,28,32]. A list of selected organic/inorganic binders is provided in Table 1.

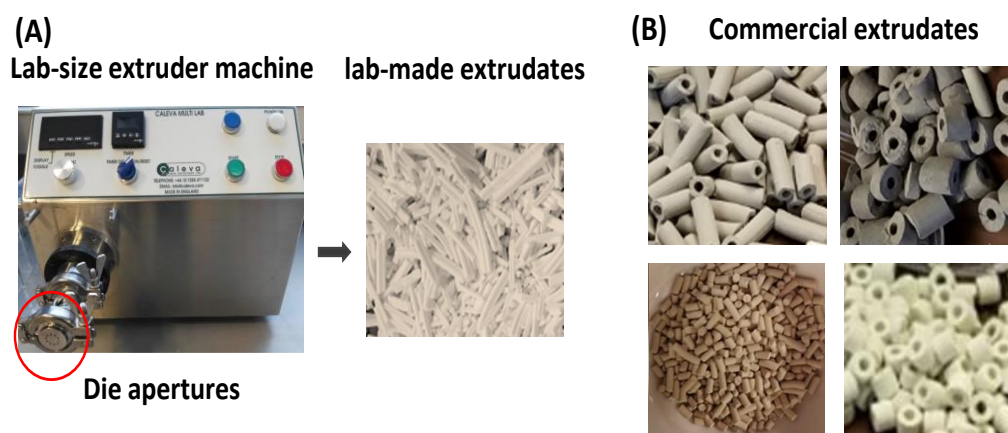


Figure 1. (A) Schematic illustration of zeolite shaping using extrusion technique, (B) Commercial extrudates with different geometrical structures.

In addition to binders and the above-mentioned additives, peptizing agents such as nitric acid can be utilized to stabilize particles and prevent their agglomeration and aid in better dispersion of binder particles in the zeolite-binder matrix [3,33]. Peptizing agents are also used to set the pH far as a point zero charge in order to prevent agglomeration of the paste [3]. In fact, large zeta potentials are known to stabilize the dispersion of particles by creating repulsion forces between positively charged particles and granting the paste mixture long-term suspension stability, consequently decreasing the viscosity of the paste [3,34]. To obtain a highly homogenized paste mixture, high degrees of mixing and stirring have been also recommended [34]. During the extrusion, the rheological behavior of primary paste is a crucial parameter impacting the ultimate mechanical stability. While a dry paste is highly viscous and can increase the possibility of the formation of cracks in the extrudates, a very wet initial paste mixture provides a very poor mechanical stability for extrudates [3,25]. To improve the rheological properties of paste parallel to final

textural properties of extrudates, different additives such as plasticizers (e.g., starch, sugars, cellulose derivatives, and mineral clays), water soluble polymers (e.g., polyethylene glycol, poly vinyl alcohol), organic porogens (e.g., carbon black, starch, or organic fillers), and lubricants and peptizing additives (e.g., dilute nitric or acetic acids) are added to produce a low viscous paste displaying a lower frictional behavior and, thus, less crack in the final extrudates [3,34–37]. Calcination, which is the last step for obtaining final extrudates from green extrudates (i.e., before thermal treatment at high temperatures), can enhance the strength of extrudates and make them more mechanically stable through agglomeration of dealuminated sections inside the extrudates [18,38]. Poor mechanical strength leads to catalyst malfunction and significant pressure drop in packed beds, owing to dust formation. Several techniques for the mechanical strength measurement of shaped bodies have been developed, such as crushing, knife edge cutting, and three-point ending [39]. However, the single pellet crushing strength test has been generally accepted as a standard technique for this measurement [40]. By testing different geometries such as spheres, cylindrical tablets, and cylindrical and trilobe extrudates that have been subjected to mechanical strength measurement with the above-mentioned methods, it was reported that the geometry of shaped bodies is strongly determinative for the selection of measurement techniques to obtain a reliable assessment of mechanical stability. For instance, both crushing and cutting tests are appropriate for tablets [39], while for extrudates cutting and bending, and for spherical shaped bodies crushing test is more practical [39]. More details can be found in a previously cited reference [41].

Table 1. A list of selected organic/inorganic binders.

Entry	Zeolite Type	Organic Binder	Inorganic Binder	Ref.
1	3A	Copolymer (ethylene/butyle acrylate, 17 wt% and 30 wt% copolymer)	-	[31]
2	3A	Polyethylene	-	[31]
3	Y	Cellulose fibers	-	[32]
4	TiO ₂ monolith	Polyethylene and methyl-hydroxyl-cellulose	Bentonite, glass fiber	[42]
5	ZSM-5		Aluminum phosphate γ -Al ₂ O ₃	[28]
6	X, Y, ZSM-12, Mordenite, zeolite A, P, ZSM-5, MCM-41	-	Portland cement, High Al cement Sulphoaluminate cements, phosphate, bonded cements, blast furnace slag cements, Ca ₃ SiO ₅ , (Ca ₂ SiO ₄), alumino-ferrite, tricalcium aluminate, calcium aluminates such as monocalcium aluminate (Ca ₃ Al ₂ O ₆), and calcium hexoaluminate (CaAl ₂ O ₄), used alone or as a mixture	[29]
7	ZSM-5	-	α -Alumina monohydrate	[30]
8	ZSM-5	Cellulose	Catapal D (Boehmite alumina)	[34]
9	5A	carboxymethylcellulose	Kaolin	[43]
10	ZSM-5	-	Silica/Alumina	[36]
11	ZSM-5, 11, 23, 35, 38, 48, Beta, X, Y, L	-	Silica	[44]

Although other shaping technologies such as granulation, spray drying, wet or dry pressing, and pelletizing are well-known industrial techniques [35,45], extrusion is the most applicable method at the industrial level due to its high capacity and low preparation costs as well as other advantages such as narrow distribution of particle size and diversity in geometries [3,34,35]. In contrast to shape diversity in extrusion, only spherical bodies are produced by granulation or spray drying where their average particle size is in the range

between 1 mm to 20 mm for granulation and 10 μm to 100 μm for spray drying [34,45]. For instance, high Resolution Scanning Electron Microscopy (HRSEM) and Focused Ion Beam Scanning Electron Microscopy (FIB-SEM) are two imaging techniques used for the structural study of extrudates and proved this uniformity, which has been attributed to two different agglomeration mechanisms taking place during extrusion or granulation [46].

2.1. The Important Parameters in Rheological Behavior of Extrudates

The rheological behavior of primary paste is determined on the empirical basis, and it aims to produce low viscous paste displaying lower frictional behavior and, thus, lesser cracks in the final extrudates. Peptizing agents are usually used for setting the pH to the target point of zero charge and prevent agglomeration of the paste [34]. Another important parameter is zeta potential (i.e., isoelectric potential in colloidal chemistry), and it is known that large zeta potentials stabilize the dispersion of particles by creating repulsive forces between positively charged particles and decrease the viscosity of the paste mixture [3,34]. Herein, zeta potential is an indicator of long-term suspension stability [3].

As mentioned before, adjusting water content during paste preparation is a critical factor to provide low viscous but sufficiently adhesive paste, which is easily shaped into noodles when passing through the die apertures. This occurs as a result of high shear stress in the extrusion chamber, as depicted in Figure 2. The shear stress is described by Equation (1):

$$\tau = \tau_0 + k \cdot \gamma^n \quad (1)$$

in which, τ is the shear stress (Pa), τ_0 is the minimum stress (the quantity that a substance can easily flow above this point), k is the consistency coefficient (Pa.sn), γ is the shear rate (Pa/s), and n is the flow index. For $n = 1$, Newtonian fluid properties are observed, while for $n < 1$, fluid displays Thixotropic behavior, and, for $n > 1$, shows dilatants behavior.

In addition, viscosity can be measured based on Equation (2) [30],

$$\eta = k \cdot \gamma^{n-1} \quad (2)$$

which can be reformulated in the form of Equation (3) as follows [3]:

$$\eta = \frac{\tau_0}{\gamma} + k \cdot \gamma^{n-1} \quad (3)$$

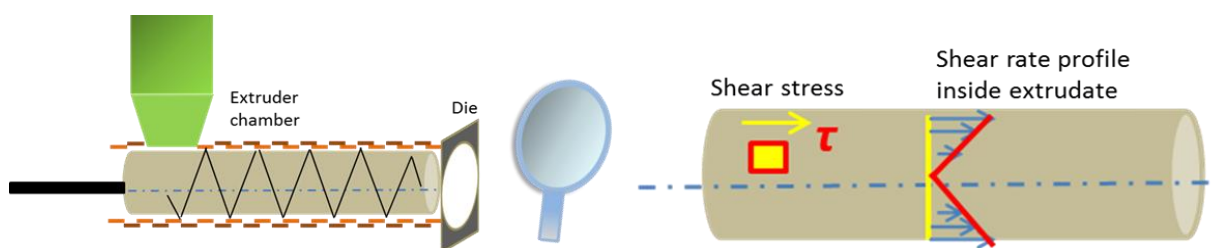


Figure 2. Shear stress (τ) applied to the extrudates during extrusion and shear rate profile on the extrudates.

Based on the Herschel–Bulkley model, both shear stress and the viscosity of the paste passing through the extrusion chamber will depend on the shear rate imposed on the paste mixture [28]. A flow index close to zero shows plug flow properties, which are known as the ideal flow regime, but the flow behavior of the paste is close to 0.7, which fundamentally indicates non-Newtonian fluid behavior [3,36,42]. When the paste is passing through the die, different radial velocity profiles are generated. If the velocity index is significant in the radial axis, extruded noodles will possess macro-defects, particularly macro-cracks [36]. Furthermore, inside the extrusion chamber, appropriate zeta potentials separate the moving phase of the paste from the stationary phase, which is attached to the

surfaces of the chamber and allows the moving phase to flow freely [42]. The zeta potential can be obtained from Henry's equation as follows [47]:

$$\zeta = \frac{3\eta U_e}{2\varepsilon f(Ka)} \quad (4)$$

in which ζ is zeta potential, η is viscosity of paste, U_e is electrophoretic mobility, ε is the dielectric constant, and $f(Ka)$ is the Henry's function with values of 1.0 or 1.5 [47]. Finally, the relation between shear yield stress and zeta potential is shown in the following equation [36,48]:

$$\tau_0 = \tau_{0,max} + k_0 \tau_{0,max} \zeta^2 \quad (5)$$

where $\tau_{0,max}$ is the maximum shear stress at zeta potential of zero and k_0 is a specific constant for the system. More details about binder content, its influence on shear yield stress, and the role of additives such as poly vinyl alcohol to adjust proper zeta potential can be found elsewhere [49]. Setting the zeta potential at a value where the best dispersion for the paste mixture is obtained dedicates the mechanical stability, reduces defects at the end of the process, and prevents the formation of agglomerated areas inside the final extrudates. Modification of zeta potential so that the paste will behave close to a Newtonian fluid should be prevented as it leads to lesser shape integrity [3].

2.2. Binder Effects on Zeolite Physicochemical Properties

Binders have different physicochemical properties compared with pure zeolites and, thus, the presence of a binder can adversely affect the zeolite textural, adsorption, and catalytic properties. It has been reported that commercial binder-containing 5A zeolite has a lower adsorption capacity for n-paraffins compared to the pure powder of 5A zeolite [50]. Like zeolite, the binder can also adsorb molecules and change the polar interaction between adsorbate and zeolite surface, leading to the reduction of adsorption heat and a higher coalescing factor between adsorbed molecules and active sites [43,50]. From a textural point of view, the porosity and surface area of shaped zeolites is affected by the binder materials, particularly those that have different particle size and, remarkably, a lower surface area than zeolite, which, in turn, results in pore blockage and the reduction of the surface area. The generation of larger meso- and macropores in the extrudates depends on the size of the binder particles (which is around 10 nm in the case of silica or alumina binders) [28]. Furthermore, the presence of additional porosity inside the extrudates is highly dependent on the degree of the porosity of the binder. A more closely connected network in the final extrudates is created using binders with smaller particle sizes (e.g., silica, alumina, or boehmite) while the larger degrees of interparticle porosities are generated by binders with large-size particles, such as plate-like kaolin [25,51]. From a chemical alteration point of view, dilution of acidic centers of zeolite, variation in their sorption/catalytic properties, and migration of undesired cations or impurities from binder to zeolite might also occur in the course of the extrusion step. For example, the ZSM-5 extrudates prepared with different binders such as boehmite, attapulgite, and silica displayed a lesser amount of the Brønsted acidity as proved by FTIR spectroscopy analysis [25], but kaolin did not show any chemical interaction with ZSM-5, and the kaolin containing ZSM-5 displayed acidic properties close to pure ZSM-5 [25]. Similar observation has been cited for H-gallosilicate and ascribed to the consequence of zeolite partial neutralization through ion-exchange of active sites of zeolite with mobile ions (e.g., alkali or alkaline earth cations such as Na^+ or Mg^{2+}) of binders, and dealumination was also proved by ^{27}Al MAS NMR analysis [52]. In contrast, insertion of alumina as a binder can produce extra acid sites inside the zeolite extrudates [30]. For instance, in a study, the effect of alumina binder was investigated on the zeolite acidic properties using UV/Vis and confocal fluorescence microspectroscopy and demonstrated the migration of Al species from the alumina binder into the ZSM-5 extrudates [53]. These Al species are tetrahedrally coordinated into the zeolite framework and thus increase the amount of zeolite Brønsted acidity [53]. Higher catalytic activities

for ZSM-5 extrudates have been previously reported when alumina was used as a binder in acid-catalyzed reactions (e.g., n-hexane cracking, propylene oligomerization, lube oil dewaxing, and methanol conversion to hydrocarbons) [44]. In addition, the influence of the alumina binder in the enhancement of the catalytic activity of ZSM-5 extrudates have been formerly admitted in several acid-catalyzed reactions [44]. However, the catalytic activity of zeolite/alumina matrix did not display an increasing trend when they were dry-mixed in the absence of water proved that the wet zeolite/alumina phase is prone to the generation of additional Brønsted acid centers in the final composite [44]. In addition, several studies have been performed to determine the effect of different binders on zeolite acidity, and more details can be found elsewhere [54–62]. This evidence demonstrates that the choice of proper materials as binder agents is not identical for different cases and highly depends on the binder interaction with zeolites as well as its effects on the physicochemical properties of zeolite for a given reaction [44,63,64]. The non-uniform distribution of binders inside the extrusion mixture can generate chemically different zones. While rich zeolite zones (e.g., those parts with lesser binder content) inside the extrudates increase the reaction rate, rich binder-containing zones show much lower catalytic activity, which leads to lower reproducibility in the catalytic/adsorption performance of different batches of extrudates. Owing to the different textural and chemical structures in the two inhomogeneous zones, the reaction rate is controlled by mass transfer rather than by kinetics [56]. However, the solid state ion-exchange, due to the close contact of zeolite and the binder, has displayed two-sided effects, including both positive and negative outcomes such as neutralization of active sites, Si and Al migration, and poison trapping [57].

3. Zeolites Shaping Using Alternative Binder-Free Techniques

Because of the possible negative impacts of binders on zeolite properties, as explained previously, many studies have been conducted to develop binder-free alternative methods for zeolite structuring. Although some early studies have been conducted by Universal Oil Products Company (UOP) [65,66], more recently, different and new methods such as hard templating technique, hydrothermal transformation, pulsed current [67], and some other novel processes [68] have been tested for structuring zeolite particles using binder-free technologies. Amongst them, the hard templating technique and hydrothermal transformation are discussed in detail in the coming sections of this paper. The ultimate shape and geometry of binder-less zeolitic structures is almost identical to binder-containing analogous (e.g., spheres, cylinders, hollow cylinders, honeycombs, etc.) but they are prepared in the absence of any binder agent. The additional additives utilized during the shaping step (e.g., organic materials) are combusted and removed by thermal treatments, therefore, final structured zeolite bodies can contain up to 100% pure zeolite particles.

3.1. Macroscopic Hard Templating Casting

Macroscopic-size and porous hard templates are generally applied to generate both larger porosity in zeolite as well as to structure them simultaneously. Indeed, the hard templating technique is a casting method used to produce porous zeolitic bodies by immersing a solid template in the primary mixture of zeolite initiators. The zeolite particles are crystallized inside the pores of the template, and after solidification by hydrothermal treatment and following drying, the template is removed by calcination at an elevated temperature and a zeolitic body that is texturally a replica of the original template remains. A wide range of hard templates, such as polystyrene spheres [69], latex beads [70] and carbon materials (e.g., monoliths, fibers or disks) [71], have been applied as hard templates to shape the zeolites. For instance, binder-free silicalite-1 spheres were synthesized using ion-exchange resin beads as macroscopic hard templates [72]. After resin removal by calcination, hierarchically porous and spheres with the particle diameter in a range between 0.4 and 0.85 mm remain (Figure 3).

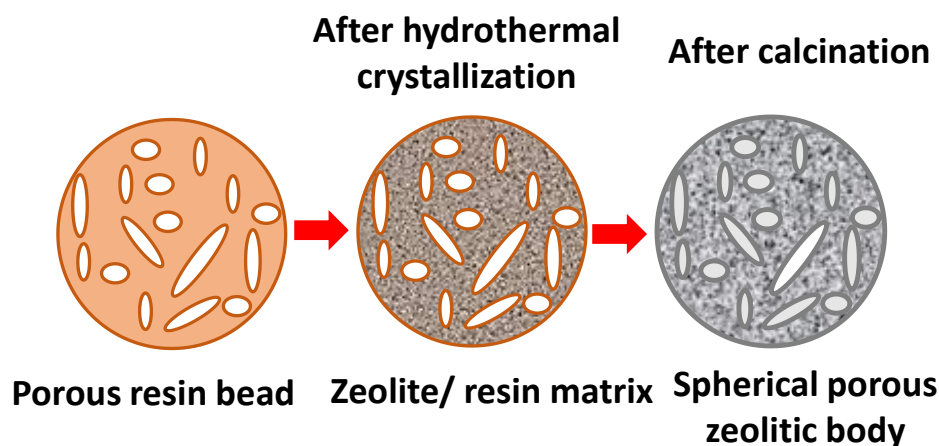


Figure 3. Synthesis of bead shape silicalite-1 using resin beads as hard templates.

Afterwards a series of zeolites in bead format were synthesized using this technique (e.g., zeolite Beta and ZSM-5) and metal-containing zeolite beads (e.g., Cr- and Pd-Beta) have also been synthesized in bead format [73–76]. Other porous solids such as organic aerogel, Polyurethane foams (PUFs) [77], carbon materials [78], and natural bio-based materials [79] have also been used as hard templates to shape zeolites. Some examples are: spongy silicalite obtained using starch and hierarchical silicalite-1 and Beta synthesized using aerogels as hard templates [77–79]. A list of different zeolitic frameworks in the spherical format as discussed above is summarized in Table 2.

Table 2. Summary of properties of synthesized zeolite beads.

Entry	Type of Zeolite Framework	Commercial Name of Resin	Si/Al Ratio	Surface Area (m ² /g)	Application	Ref.
1	Silicalite-1/MFI	MSA-1	∞	930	Catalysis/Molecular Sieve	[72]
2	Silicalite-1/MFI	WBA	∞	559	Catalysis/Molecular Sieve	[72]
3	Beta/BEA	MSA-1	50	640	Catalysis	[73]
4	ZSM-5/MFI	MSA-1	50	300–850	Catalysis	[74]
5	Cr-Beta/BEA	MSA-1	50	651	Catalysis	[75]
6	Pd-Beta/BEA	MSA-1	50	144	Catalysis	[76]

3.2. Hydrothermal Transformation

By means of hydrothermal transformation, a temporary binder mixed with zeolite powder, is converted to the zeolitic phase in the course of hydrothermal treatment. In addition to this, non-zeolitic materials (e.g., different types of clays or silica) can be transformed into zeolitic frameworks. The latter transformation needs an aqueous medium and, practically, a partial autogenic hydrothermal condition. By means of this method and in the presence of organic fillers such as cellulose, zeolites Y, X and A have been obtained by binder transformation inside the pre-fabricated bodies [80]. In addition, some inorganic materials such as silica or mineral clays such as kaolin and metakaolin have been converted into different zeolite frameworks (e.g., MFI, BEA, FAU) by aging them in an alkaline medium (OH/SiO₂ molar ratio up to 1.2), and they showed acceptable mechanical stability [81]. Clay minerals such as kaolin or metakaolin and silica consist of similar elements that are present in zeolites (e.g., Si, Al, Na), and they can thus be utilized as the resource of starting materials to initiate zeolite formation and following crystallization propagation. It has been reported that by means of a three-step hydrothermal conversion, kaolin extrudates can be transformed to silica X [80]. In addition, zeolite X, A, and mor-denite have been obtained through the conversion of metakaolin (the activated form of kaolin prepared by kaolin thermal activation at 973 K) [81,82]. Next, using a mixture of NaOH, KOH, distilled water, and metakaolin, agitated for a maximum of 10 days, a 100% crystalline zeolite phase was obtained [81]. The alkaline solution is used as a mineralizer

to assist the conversion of non-zeolitic materials to binder-free zeolite bodies. More details can be found in the previously cited literature [83]. Another class of pre-fabricated materials are glassy substances and, in this context, porous glass beads and glassy granules were transformed to MFI beads and to ZSM-5 granules, respectively [84,85]. Likewise, zeolite A tubes have been also synthesized, but, in this case, crystalline structures with large macropores in the range of 3 μm were obtained [86]. In addition, silicalite-1 disk has been synthesized by transformation of a kanemite disk (a single-layer silicate) using triphenylamine (TPA) cation by phase separation under a dry treatment (or so-called dry solid-state transformation) [87]. This technique is involved with gradual dissolution of bulk material (so-called BMD) resulting in zeolite monolith formation [88]. For instance, tubular zeolite monoliths with MFI topology were obtained by direct conversion of porous glass materials [88]. The BMD technique is based on the direct conversion of raw materials into zeolites under static conditions. This technique can be also conducted under a stirring condition, which is known as dynamic bulk material dissolution (DBMD). By employing the BMD technique and adjusting the solubility of precursors, zeolite tubular bodies have been obtained (Figure 4).

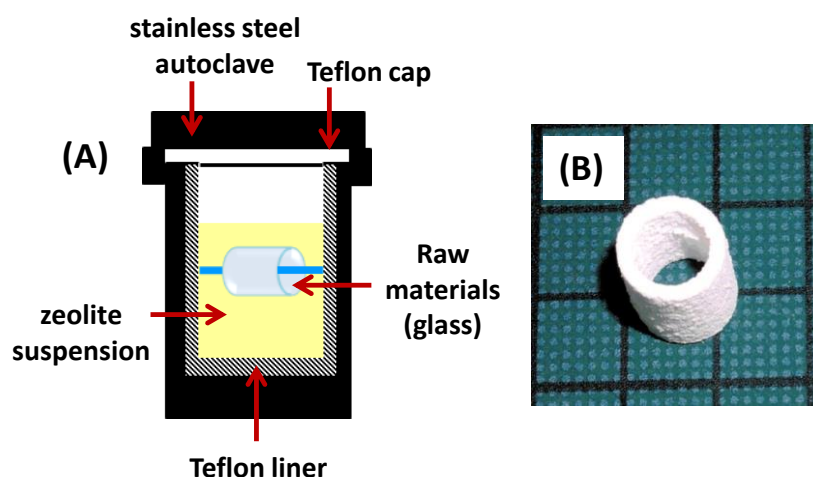


Figure 4. (A): Schematic illustration of the synthesis route for bulk material dissolution technique under static condition; (B): obtained monolith [87].

By means of this technique, a tubular and porous quartz glass was gradually converted to a MFI framework. The transformation reaction took place by inserting quartz glass in an autoclave equipped with polytetrafluoroethylene (PTFE) liner. In addition, other reagents such as tetrapropylammonium hydroxide (TPAOH), hydrogen fluoride (HF), and about 50 mg of MFI zeolite seeds were added to this mixture and stirred under 10 rpm at 200 °C for 61 days. From the point of view of the formation mechanism, a gradual formation of the MFI phase took place and was followed by a very moderate growth of MFI crystals, which propagated from the surface of the quartz toward the inside of the quartz body and gradually converted the glassy SiO_2 species to the MFI phase, and this led to that zeolite entirely replaced the quartz [88]. Here, seeds of MFI as initiators form new nuclei to trigger the formation of primary MFI building blocks and accelerate the crystallization process under a very slow stirring rate. Based on the selected conditions of this technique, partially transformed fibers and fabrics have also been obtained [88]. The drawbacks of this technique are the need for a large amount of time for the conversion of inorganic materials into zeolite, and, in some cases, the formation of a non-homogeneous composite consisting of the zeolite phase and other raw material phases has been observed [88].

Other techniques such as dry sol-gel transformation and solid-state transformation have been also studied in order to synthesize binder-free zeolitic bodies including binder-free ZSM-11 and mordenite pellets obtained in a low water medium [89] as well as ZSM-5 disks obtained by the conversion of amorphous aluminosilicate fibers using solid-state

transformation [90]. Other structures such as MFI disks and films have been fabricated from primary aluminosilicate glasses using a solid-state transformation followed by the phase separation under hydrothermal treatment [86,90].

One interesting alternative is the pseudomorphic transformation of raw materials with the possibility to optimize the morphology of shaped zeolites. Using this technique, spherical Alginate/zeolite and alginate/zeolite-bentonite composite have been obtained, as depicted in Figure 5 [91]. In addition, pre-shaped zeolite Y/alginate spheres have been also transformed into pure zeolite Y with the same geometrical appearance (i.e., pre-shaped spheres) [91]. Following calcination at 600 °C for 44 h and decomposition of alginate, the binder-free zeolite granules were obtained [91].

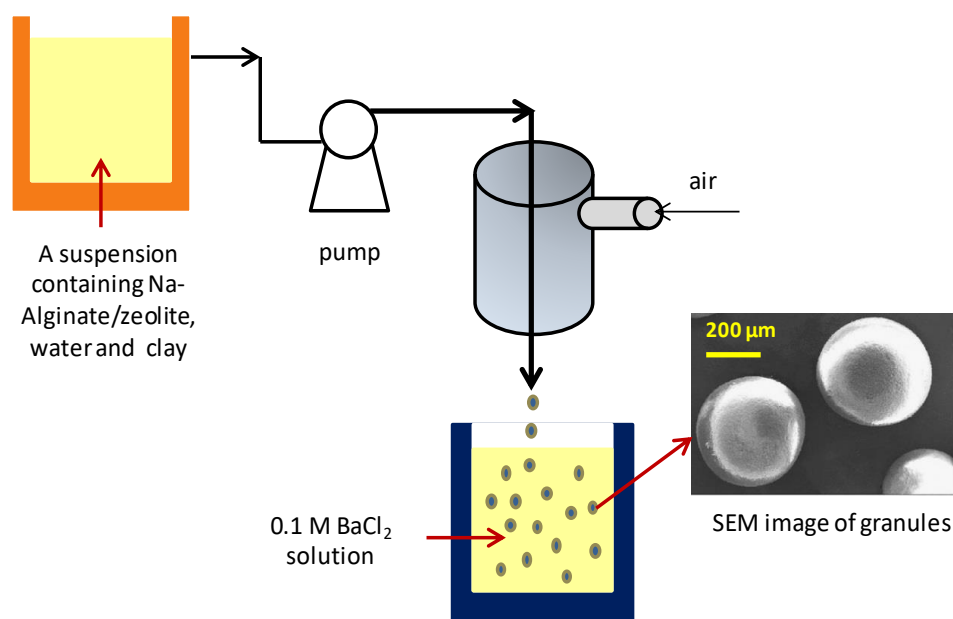


Figure 5. Schematic representation of synthesis granular and binder-free zeolite Y [91].

Other frameworks such as sodalite (SOD), Linde Type A (LTA) and faujasite X (FAU-X) have also been prepared by pseudomorphic transformation [92]. A type of hierarchical zeolite Beta monoliths have also been obtained through a layer-by-layer process using silica gel transformation [93], for which more details about the properties and synthetic routes can be found in previously cited literatures [92,93]. All these transformation techniques have a multi-step synthetic procedure for obtaining zeolite bodies. Recently, a one-step in situ hydrothermal synthesis has been developed in which silica sol was suspended in an oil/water system (immiscible liquids system) and granular zeolite A has been obtained by silica sol transformation (Figure 6) [94]. In this synthesis, heptane was used as the oil phase while the aqueous phase was a mixture of sodium aluminate, NaOH, and deionized (DI) water. Silica sol was gradually dropped into the oil phase and, over time, Al species slowly diffused to the spherical silica particles. Consequently, more silica precursors were gently dissolved in the reaction medium to release more Si species and push forward the nucleation step. Indeed, Al species were attached to the Si species via oxygen bridges in a way that these species produced the zeolite primary building blocks. This synthesis route was involved with the sol suspension inside of two immiscible phases and further followed by the next gelation step. The full conversion of silica to zeolite was completed during the hydrothermal crystallization inside the alkaline solution. As mentioned above, clay extrudates can be also converted in an alkaline pH into zeolites. Zeolite A, X and MFI have also been obtained using this technique and alkaline pH [94]. The average diameter of the shaped particles is in the millimeter range, but a wide particle size distribution was observed.

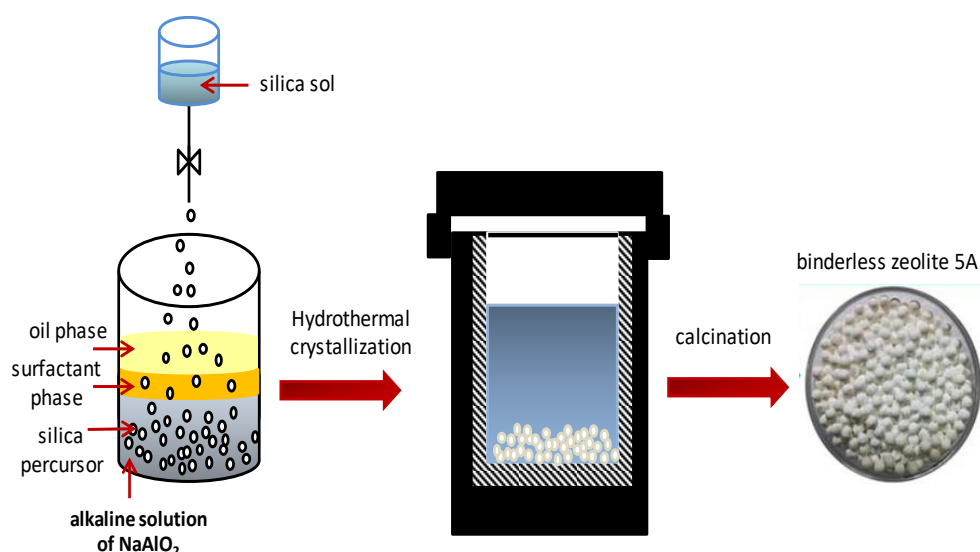


Figure 6. Schematic illustration of one-step synthesis protocol for preparing binder-free granules of zeolite A [94].

As the last case study, a one-pot template- and a binder-free synthesis route for obtaining shaped mordenite under an acid-hydrolysis condition is reviewed here. By means of this technique, primary species were converted into the hierarchical and mechanically strong mordenite bodies during the hydrothermal crystallization [95]. In a typical synthesis, TEOS (tetraethyl orthosilicate as silica precursor) was dissolved in demineralized water (DI), and, next, HCl was slowly added to the mixture, which further followed by stirring for 24 h at 20 °C to thoroughly fulfill the hydrolysis step. The Al precursor was obtained by mixing aluminum sulfate ($\text{Al}_2(\text{SO}_4)_3$), sodium hydroxide (NaOH), and DI water with pre-defined molar ratios. Silica mixture was added to Al solution, entirely mixed, and aged for 24 h at room temperature. Finally, the resultant mixture was transferred to a Teflon-lined stainless steel autoclave and hydrothermally heated for preselected times at 170 °C (Figure 7) [95]. The highest degree of crystallinity and mechanical stability was observed after 144 h hydrothermal heating. At the end, mordenite monoliths with cubic or cylindrical structures with high mechanical strengths were obtained without any shrinkage by calcination at 550 °C. The obtained structured mordenite were used as catalysts in a Friedel–Crafts benzylation reaction of benzene with benzyl alcohol, and showed higher activity compared with the powder analogue. From a mechanical strength point of view, these monoliths were reported to be close to industrially available counterparts, and thereby, they show promising performance for industrial applications.

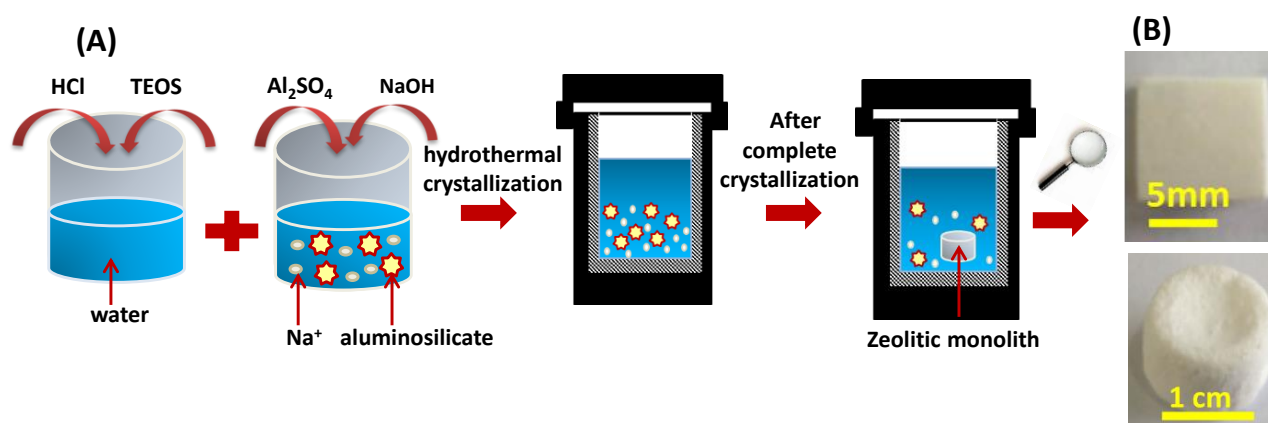


Figure 7. (A): Schematic illustration of one-step template- and binder-free synthesis route for preparing mordenite monoliths, (B): obtained monoliths with different shape geometries [95].

4. Conclusions, Recommendations and Future Perspectives

The shaping of zeolites is a complex task that entails several considerations such as mass transfer prerequisites, pressure drop prevention, cost, and stability investigations [96–98]. The present review provides an outline of different shaping techniques as well as their possible effect on the physicochemical properties of structured bodies, as highlighted in different sections. Each technique has its own impact on the original physicochemical properties of zeolite, which are discussed thoroughly in the context of this review. Extrusion is a common industrial technique in which binders (e.g., silica, alumina, or clays) are employed to increase mechanical stability. Hence, they might have their own so-called side-effects on basic features of zeolites, so that some of these effects are undesired or detrimental. Some of them, as mentioned before, involve a change in the adsorption properties of binder-containing zeolites, which may reduce relative to the increase in binder quantity. Other major drawbacks frequently observed for several binders are neutralization of active sites and partial pore blockage, and, consequently, a decrease in the surface area. Regarding the probable disadvantages of binders, alternative methods have been investigated and showed a possible capacity to diminish binder drawbacks by higher degrees of preservation of the inherent physicochemical properties of the zeolites. However, the downside of these techniques is the lower mechanical strength, which is more pronounced for the hard templating approach. It is noteworthy that binder selection is a function of different parameters, such as specific applications and their requirements, and, thus, is a trade-off between inhibiting and promoting results in different cases. With a critical look at how shaping techniques have been developed in recent decades, a forward progress trend is obvious by several numbers of patents and research delivered each year to the public. However, looking to the future, there is still a need for the development and refinement of available techniques, in particular, with a combination of new computational techniques with experimental results. Evidently, more accurate and realistic criteria should be defined for preserving original properties of zeolites after shaping, and might need to seek more adapted technologies. Despite the limitations and reported downsides, binder-free alternatives proved to be an applicable method for retaining the original properties in shaped zeolites, but the scale-up feasibility is still ongoing and requires comprehensive study.

Author Contributions: Conceptualization, Z.A.P. and K.O.S.; methodology, Z.A.P., L.C. and K.O.S.; formal analysis, Z.A.P., Y.A.A. and K.O.S.; investigation, Z.A.P., M.M.A. and K.O.S.; writing—original draft preparation, Z.A.P. and K.O.S.; writing—review and editing, Z.A.P., P.H.M.V.S. and K.O.S.; visualization, Z.A.P. and K.O.S.; supervision, K.O.S. All authors have read and agreed to the published version of the manuscript.

Funding: This research received no external funding.

Data Availability Statement: Not applicable.

Acknowledgments: The authors would like to sincerely thank both the University of Groningen, Netherlands and the Laboratory for Chemical Technology (LCT), Ghent University, Belgium.

Conflicts of Interest: The authors declare no conflict of interest.

References

1. Ergun, S. Fluid flow through packed columns. *Chem. Eng. Prog.* **1952**, *48*, 89–94.
2. Foumeny, E.A.; Kulkarni, A.; Roshani, S. Elucidation of pressure drop in packed-bed systems. *J. Appl. Therm. Eng.* **1996**, *16*, 195–202. [[CrossRef](#)]
3. Devyatkov, S.; Kuzichkin, N.V.; Murzin, D.Y. On Comprehensive Understanding of Catalyst Shaping by Extrusion. *Chim. Oggi-Chem. Today* **2015**, *33*, 57–64.
4. De Wind, M.; Plantenga, F.L.; Heinerman, J.J.L.; Free, H.W.H. Upflow versus Downflow Testing of Hydrotreating Catalysts. *Appl. Catal.* **1988**, *43*, 239–252. [[CrossRef](#)]
5. Corma, A.; Martinez, A. Zeolites and Zeotypes as Catalysts. *Adv. Mater.* **1995**, *7*, 137–144. [[CrossRef](#)]
6. Asgar Pour, Z.; Sebakhy, K.O. A Review on the Effects of Organic Structure-Directing Agents on the Hydrothermal Synthesis and Physicochemical Properties of Zeolites. *Chemistry* **2022**, *4*, 431–446. [[CrossRef](#)]

7. Rabo, J.A.; Schoonover, M.W. Early Discoveries in Zeolite Chemistry and Catalysis at Union Carbide, and Follow-up in Industrial Catalysis. *Appl. Catal. A Gen.* **2001**, *222*, 261–275. [\[CrossRef\]](#)
8. Tanabe, K.; Hölderich, W.F. Industrial Application of Solid Acid–Base Catalysts. *Appl. Catal. A Gen.* **1999**, *181*, 399–434. [\[CrossRef\]](#)
9. Dapsens, P.Y.; Mondelli, C.; Pérez-Ramírez, J. Design of Lewis-Acid Centres in Zeolitic Matrices for the Conversion of Renewables. *Chem. Soc. Rev.* **2015**, *44*, 7025–7043. [\[CrossRef\]](#)
10. Ch Deka, R. *Acidity in Zeolites and Their Characterization by Different Spectroscopic Methods*, 5th ed.; Indian Journal of Technology: New Delhi, India, 1998.
11. Moshoeshoe, M.N.; Nadiye-Tabbiruka, M.S.; Obuseng, V.C. A Review of the Chemistry, Structure, Properties and Applications of Zeolites. *Am. J. Mater. Sci.* **2017**, *7*, 196–221.
12. Primo, A.; Garcia, H. Zeolites as Catalysts in Oil Refining. *Chem. Soc. Rev.* **2014**, *43*, 7548–7561. [\[CrossRef\]](#)
13. Davis, M.E. Ordered Porous Materials for Emerging Applications. *Nature* **2002**, *417*, 813–821. [\[CrossRef\]](#)
14. Corma, A. From Microporous to Mesoporous Molecular Sieve Materials and Their Use in Catalysis. *Chem. Rev.* **1997**, *97*, 2373–2420. [\[CrossRef\]](#)
15. Mintova, S.; Gilson, J.-P.; Valtchev, V. Advances in Nanosized Zeolites. *Nanoscale* **2013**, *5*, 6693–6703. [\[CrossRef\]](#)
16. Lakiss, L.; Gilson, J.P.; Valtchev, V.; Mintova, S.; Vicente, A.; Vimont, A.; Bedard, R.; Abdo, S.; Bricker, J. Zeolites in a good shape: Catalyst forming by extrusion modifies their performances. *Microporous Mesoporous Mater.* **2020**, *299*, 110114. [\[CrossRef\]](#)
17. Wang, Y.; Chang, Y.; Liu, M.; Zhang, A.; Guo, X. A facile strategy to prepare shaped ZSM-5 catalysts with enhanced para-xylene selectivity and stability for toluene methylation: The effect of in situ modification by attapulgite. *Molecules* **2019**, *24*, 3462. [\[CrossRef\]](#)
18. Perego, C.; Villa, P. Catalyst Preparation Methods. *Catal. Today* **1997**, *34*, 281–305. [\[CrossRef\]](#)
19. Pérez-Ramírez, J.; Mitchell, S.; Verboekend, D.; Milina, M.; Michels, N.-L.; Krumeich, F.; Marti, N.; Erdmann, M. Expanding the Horizons of Hierarchical Zeolites: Beyond Laboratory Curiosity towards Industrial Realization. *ChemCatChem* **2011**, *3*, 1731–1734. [\[CrossRef\]](#)
20. Verboekend, D.; Mitchell, S.; Pérez-Ramírez, J. Hierarchical Zeolites Overcome All Obstacles: Next Stop Industrial Implementation. *Chimia* **2013**, *67*, 327. [\[CrossRef\]](#)
21. Michels, N.-L.; Mitchell, S.; Milina, M.; Kunze, K.; Krumeich, F.; Marone, F.; Erdmann, M.; Marti, N.; Pérez-Ramírez, J. Hierarchically Structured Zeolite Bodies: Assembling Micro-, Meso-, and Macroporosity Levels in Complex Materials with Enhanced Properties. *Adv. Funct. Mater.* **2012**, *22*, 2509–2518. [\[CrossRef\]](#)
22. Beeckman, J.W.L.; Fassbender, N.A.; Datz, T.E. Length to diameter ratio of extrudates in catalysis technology I. Bending Strength versus impulsive forces. *AIChE J.* **2016**, *62*, 2658–2669. [\[CrossRef\]](#)
23. Gustafson, W.R.; Conn, T. Shaped Catalyst Particle. US Patent 3,966,644, 29 June 1967.
24. Hagen, J. Catalyst Shapes and Production of Heterogeneous Catalysts. *Ind. Catal.* **2015**, 211–238. [\[CrossRef\]](#)
25. Michels, N.-L.; Mitchell, S.; Pérez-Ramírez, J. Effects of Binders on the Performance of Shaped Hierarchical MFI Zeolites in Methanol-to-Hydrocarbons. *ACS Catal.* **2014**, *4*, 2409–2417. [\[CrossRef\]](#)
26. Jasra, R.V.; Tyagi, B.; Badheka, Y.M.; Choudary, V.N.; Bhat, T.S.G. Effect of Clay Binder on Sorption and Catalytic Properties of Zeolite Pellets. *Ind. Eng. Chem. Res.* **2003**, *42*, 3263–3272. [\[CrossRef\]](#)
27. Tischer, R.E. Preparation of Bimodal Aluminas and Molybdena/Alumina Extrudates. *J. Catal.* **1981**, *72*, 255–265. [\[CrossRef\]](#)
28. Freiding, J.; Patcas, F.-C.; Kraushaar-Czarnetzki, B. Extrusion of Zeolites: Properties of Catalysts with a Novel Aluminium Phosphate Sintermatrix. *Appl. Catal. A General.* **2007**, *328*, 210–218. [\[CrossRef\]](#)
29. Bazer-Bachi, D.; Harbuzaru, B.; Lecolier, E. Zeolite Formed by Extrusion and Pelleting with a Hydraulic Binder Having Improved Mechanical Properties and Process and Preparing Same. U.S. Patent 20,160,288,109A1, 6 October 2016.
30. Shihabi, D.S.; Garwood, W.E.; Chu, P.; Miale, J.N.; Lago, R.M.; Chu, C.T.-W.; Chang, C.D. Aluminum Insertion into High-Silica Zeolite Frameworks: II. Binder Activation of High-Silica ZSM-5. *J. Catal.* **1985**, *93*, 471–474. [\[CrossRef\]](#)
31. Bouvier, L.; Nicolas, S.; Medevielle, A.; Alex, P. Zeolite Adsorbent Having an Organic Binder. U.S. Patent 8,932,386B2, 13 January 2015.
32. Akhtar, F.; Andersson, L.; Ogunwumi, S.; Hedin, N.; Bergström, L. Structuring Adsorbents and Catalysts by Processing of Porous Powders. *J. Eur. Ceram. Soc.* **2014**, *34*, 1643–1666. [\[CrossRef\]](#)
33. Lynn, M. Method of Making a High Strength Catalyst, Catalyst Support or Adsorber. U.S. Patent 5,633,217, 27 May 1997.
34. Whiting, G.T.; Chung, S.-H.; Stosic, D.; Chowdhury, A.D.; van der Wal, L.I.; Fu, D.; Zecevic, J.; Travert, A.; Houben, K.; Baldus, M.; et al. Multiscale Mechanistic Insights of Shaped Catalyst Body Formulations and Their Impact on Catalytic Properties. *ACS Catal.* **2019**, *9*, 4792–4803. [\[CrossRef\]](#)
35. Baldovino-Medrano, V.G.; Le, M.T.; Van Driessche, I.; Bruneel, E.; Alcázar, C.; Colomer, M.T.; Moreno, R.; Florencie, A.; Farin, B.; Gaigneaux, E.M. Role of Shaping in the Preparation of Heterogeneous Catalysts: Tableting and Slip-Casting of Oxidation Catalysts. *Catal. Today* **2015**, *246*, 81–91. [\[CrossRef\]](#)
36. Devyatkov, S.Y.; Al Zinnurova, A.; Aho, A.; Kronlund, D.; Peltonen, J.; Kuzichkin, N.V.; Lisitsyn, N.V.; Murzin, D.Y. Shaping of Sulfated Zirconia Catalysts by Extrusion: Understanding the Role of Binders. *Ind. Eng. Chem. Res.* **2016**, *55*, 6595–6606. [\[CrossRef\]](#)
37. Absi-Halabi, M.; Stanislaus, A.; Al-Zaid, H. Effect of Acidic and Basic Vapors on Pore Size Distribution of Alumina under Hydrothermal Conditions. *Appl. Catal. A Gen.* **1993**, *101*, 117–128. [\[CrossRef\]](#)
38. Mitchell, S.; Michels, N.L.; Pérez-Ramírez, J. From Powder to Technical Body: The Undervalued Science of Catalyst Scale Up. *Chem. Soc. Rev.* **2013**, *42*, 6094–6112. [\[CrossRef\]](#)

39. Li, Y.; Wu, D.; Zhang, J.; Chang, L.; Wu, D.; Fang, Z.; Shi, Y. Measurement and Statistics of Single Pellet Mechanical Strength of Differently Shaped Catalysts. *Powder Technol.* **2000**, *113*, 176–184. [\[CrossRef\]](#)
40. ASTM Committee D-32; 1985 Annual Book of ASTM Standards, vol. 5.03. American Society for Testing and Materials: New York, NY, USA, 1984.
41. Rhee, Y.W.; Guin, J.A. Preparation of Alumina Catalyst Supports and NiMo/Al₂O₃ Catalysts. *Korean J. Chem. Eng.* **1993**, *10*, 112–123. [\[CrossRef\]](#)
42. Forzatti, P.; Orsenigo, C.; Ballardini, D.; Berti, F. On the Relations Between the Rheology of TiO₂-Based Ceramic Pastes and the Morphological and Mechanical Properties of the Extruded Catalysts. In *Studies in Surface Science and Catalysis*; Delmon, B., Jacobs, P.A., Maggi, R., Martens, J.A., Grange, P., Poncelet, G., Eds.; Elsevier: Amsterdam, The Netherlands, 1998; Volume 118, pp. 787–796, ISBN 0167-2991.
43. Shams, K.; Mirmohammadi, S.J. Preparation of 5A Zeolite Monolith Granular Extrudates Using Kaolin: Investigation of the Effect of Binder on Sieving/Adsorption Properties Using a Mixture of Linear and Branched Paraffin Hydrocarbons. *Microporous Mesoporous Mater.* **2007**, *106*, 268–277. [\[CrossRef\]](#)
44. Bowes, E.; Amwell, E. Extrusion of Silica-Rich Solids. U.S. Patent 4,582,815, 15 April 1986.
45. Gleichmann, K.; Unger, B.; Brandt, A. Industrial Zeolite Molecular Sieves. *Zeolites Useful. Miner.* **2016**, *5*, 89–108. [\[CrossRef\]](#)
46. Mitchell, S.; Michels, N.L.; Kunze, K.; Pérez-Ramírez, J. Visualization of Hierarchically Structured Zeolite Bodies from Macro to Nano Length Scales. *Nat. Chem.* **2012**, *4*, 825–831. [\[CrossRef\]](#)
47. Koutsoukos, P.K.; Klepetsanis, P.G.; Spanos, N.; Somasundaran, P. *Calculation of Zeta-Potentials from Electrokinetic Data*, *Encyclopedia of Surface and Colloid Science*; CRC Press: New York, NY, USA, 2006.
48. Foundas, M.; Britcher, L.G.; Fornasiero, D.; Morris, G.E. Boehmite Suspension Behaviour upon Adsorption of Methacrylate-Phosphonate Copolymers. *Powder Technol.* **2015**, *269*, 385–391. [\[CrossRef\]](#)
49. Catalyst Fundamentals. In *Catalytic Air Pollution Control*; Wiley: Hoboken, NJ, USA, 2009; pp. 1–23, ISBN 978-1-118-39774-9.
50. Sun, H.; Shen, B.; Liu, J. N-Paraffins Adsorption with 5A Zeolites: The Effect of Binder on Adsorption Equilibria. *Sep. Purif. Technol.* **2008**, *64*, 135–139. [\[CrossRef\]](#)
51. Luna-Murillo, B.; Pala, M.; Paioni, A.L.; Baldus, M.; Ronsse, F.; Prins, W.; Bruijninx, P.C.A.; Weckhuysen, B.M. Catalytic fast pyrolysis of biomass: Catalyst characterization reveals the feed-dependent deactivation of a technical ZSM-5-based catalyst. *ACS Sustain. Chem. Eng.* **2020**, *9*, 291–304. [\[CrossRef\]](#)
52. Devadas, P.; Kinage, A.K.; Choudhary, V.R. Effect of Silica Binder on Acidity, Catalytic Activity and Deactivation Due to Coking in Propane Aromatization over H-Gallosilicate (MFI). In *Studies in Surface Science and Catalysis*; Rao, T.S.R.P., Dhar, G.M., Eds.; Elsevier: Amsterdam, The Netherlands, 1998; Volume 113, pp. 425–432. ISBN 0167-2991.
53. Whiting, G.T.; Meirer, F.; Mertens, M.M.; Bons, A.-J.; Weiss, B.M.; Stevens, P.A.; de Smit, E.; Weckhuysen, B.M. Binder Effects in SiO₂²⁻ and Al₂O₃-Bound Zeolite ZSM-5-Based Extrudates as Studied by Microspectroscopy. *ChemCatChem* **2015**, *7*, 1312–1321. [\[CrossRef\]](#) [\[PubMed\]](#)
54. Mitra, B.; Kunzru, D. Washcoating of Different Zeolites on Cordierite Monoliths. *J. Am. Ceram. Soc.* **2008**, *91*, 64–70. [\[CrossRef\]](#)
55. Lee, H.J.; Kim, J.H.; Park, D.-W.; Cho, S.J. Effect of Base Binder, Flash Calcined Hydrotalcite, in MFI Zeolite Granule: Catalytic Activity over 1-Butene Isomerization and MTO Reaction. *Appl. Catal. A Gen.* **2015**, *502*, 42–47. [\[CrossRef\]](#)
56. Du, X.; Kong, X.; Chen, L. Influence of Binder on Catalytic Performance of Ni/HZSM-5 for Hydrodeoxygenation of Cyclohexanone. *Catal. Commun.* **2014**, *45*, 109–113. [\[CrossRef\]](#)
57. Kasture, M.W.; Niphadkar, P.S.; Bokade, V.V.; Joshi, P.N. On the Catalytic Performance in Isopropylation of Benzene over H/β Zeolite Catalysts: Influence of Binder. *Catal. Commun.* **2007**, *8*, 1003–1008. [\[CrossRef\]](#)
58. Mehlhorn, D.; Valiullin, R.; Kärger, J.; Schumann, K.; Brandt, A.; Unger, B. Transport Enhancement in Binderless Zeolite X- and A-Type Molecular Sieves Revealed by PFG NMR Diffusometry. *Microporous Mesoporous Mater.* **2014**, *188*, 126–132. [\[CrossRef\]](#)
59. Kong, X.; Liu, J. Influence of Alumina Binder Content on Catalytic Performance of Ni/HZSM-5 for Hydrodeoxygenation of Cyclohexanone. *PLoS ONE* **2014**, *9*, e101744. [\[CrossRef\]](#)
60. Sánchez, P.; Dorado, F.; Fúnez, A.; Jiménez, V.; Ramos, M.J.; Valverde, J.L. Effect of the Binder Content on the Catalytic Performance of Beta-Based Catalysts. *J. Mol. Catal. A Chem.* **2007**, *273*, 109–113. [\[CrossRef\]](#)
61. Uguina, M.A.; Sotelo, J.L.; Serrano, D.P. Toluene Disproportionation over ZSM-5 Zeolite: Effects of Crystal Size, Silicon-to-Aluminum Ratio, Activation Method and Pelletization. *Appl. Catal.* **1991**, *76*, 183–198. [\[CrossRef\]](#)
62. Yang, K.; Zhang, D.; Zou, M.; Yu, L.; Huang, S. The Known and Overlooked Sides of Zeolite-Extrudate Catalysts. *ChemCatChem* **2021**, *13*, 1414–1423. [\[CrossRef\]](#)
63. Dorado, F.; Romero, R.; Cañizares, P. Hydroisomerization of N-Butane over Pd/HZSM-5 and Pd/Hβ with and without Binder. *Appl. Catal. A Gen.* **2002**, *236*, 235–243. [\[CrossRef\]](#)
64. de Lucas, A.; Valverde, J.L.; Sánchez, P.; Dorado, F.; Ramos, M.J. Influence of the Binder on the N-Octane Hydroisomerization over Palladium-Containing Zeolite Catalysts. *Ind. Eng. Chem. Res.* **2004**, *43*, 8217–8225. [\[CrossRef\]](#)
65. Michaike, E. Method for Producing Molecular Sieves Zeolite Particles. U.S. Patent 3,348,911A, 24 December 1967.
66. Michaike, E. Preparation of Crystalline Zeolite Particles. U.S. Patent 3,359,068A, 19 December 1967.
67. Vasiliev, P.; Akhtar, F.; Grins, J.; Mouzon, J.; Andersson, C.; Hedlund, J.; Bergstrom, L. Strong hierarchically porous monoliths by pulsed current processing of zeolite powder assemblies. *ACS Appl. Mater. Interfaces* **2010**, *2*, 732–737. [\[CrossRef\]](#)

68. Lu, S.; Han, R.; Wang, H.; Song, C.; Ji, N.; Lu, X.; Ma, D.; Liu, Q. Three birds with one stone: Designing a novel binder-free monolithic zeolite pellet for wet VOC gas adsorption. *Chem. Eng. J.* **2022**, *448*, 137629. [\[CrossRef\]](#)
69. Holland, B.T.; Abrams, L.; Stein, A. Dual Templating of Macroporous Silicates with Zeolitic Microporous Frameworks. *J. Am. Chem. Soc.* **1999**, *121*, 4308–4309. [\[CrossRef\]](#)
70. Dong, A.; Wang, Y.; Tang, Y.; Zhang, Y.; Ren, N.; Gao, Z. Mechanically Stable Zeolite Monoliths with Three-Dimensional Ordered Macropores by the Transformation of Mesoporous Silica Spheres. *Adv. Mater.* **2002**, *14*, 1506–1510. [\[CrossRef\]](#)
71. García-Martínez, J.; Cazorla-Amorós, D.; Linares-Solano, A.; Lin, Y.S. Synthesis and Characterisation of MFI-Type Zeolites Supported on Carbon Materials. *Microporous Mesoporous Mater.* **2001**, *42*, 255–268. [\[CrossRef\]](#)
72. Tosheva, L.; Valtchev, V.; Sterte, J. Silicalite-1 Containing Microspheres Prepared Using Shape-Directing Macro-Templates. *Microporous Mesoporous Mater.* **2000**, *35–36*, 621–629. [\[CrossRef\]](#)
73. Tosheva, L.; Mihailova, B.; Valtchev, V.; Sterte, J. Zeolite Beta Spheres. *Microporous Mesoporous Mater.* **2001**, *48*, 31–37. [\[CrossRef\]](#)
74. Tosheva, L.; Sterte, J. ZSM-5 Spheres Prepared by Resin Templating. In *Studies in Surface Science and Catalysis*; Aiello, R., Giordano, G., Testa, F., Eds.; Elsevier: Amsterdam, The Netherlands, 2002; Volume 142, pp. 183–190. ISBN 0167-2991.
75. Naydenov, V.; Tosheva, L.; Sterte, J. Chromium Containing Zeolite Beta Macrostructures. In *Studies in Surface Science and Catalysis*; Aiello, R., Giordano, G., Testa, F., Eds.; Elsevier: Amsterdam, The Netherlands, 2002; Volume 142, pp. 1449–1455, ISBN 0167-2991.
76. Naydenov, V.; Tosheva, L.; Sterte, J. Palladium-Containing Zeolite Beta Macrostructures Prepared by Resin Macrotemplating. *Chem. Mater.* **2002**, *14*, 4881–4885. [\[CrossRef\]](#)
77. Lee, Y.-J.; Lee, J.S.; Park, Y.S.; Yoon, K.B. Synthesis of Large Monolithic Zeolite Foams with Variable Macropore Architectures. *Adv. Mater.* **2001**, *13*, 1259–1263. [\[CrossRef\]](#)
78. Li, W.-C.; Lu, A.-H.; Palkovits, R.; Schmidt, W.; Spliethoff, B.; Schüth, F. Hierarchically Structured Monolithic Silicalite-1 Consisting of Crystallized Nanoparticles and Its Performance in the Beckmann Rearrangement of Cyclohexanone Oxime. *J. Am. Chem. Soc.* **2005**, *127*, 12595–12600. [\[CrossRef\]](#) [\[PubMed\]](#)
79. Tong, Y.; Zhao, T.; Li, F.; Wang, Y. Synthesis of Monolithic Zeolite Beta with Hierarchical Porosity Using Carbon as a Transitional Template. *Chem. Mater.* **2006**, *18*, 4218–4220. [\[CrossRef\]](#)
80. Flank, W.H.; Fethke, W.P.; Marte, J. Process for Preparing Molecular Sieve Bodies. U.S. Patent 4,818,508A, 4 April 1989.
81. Verduijn, J.P. Process for Producing Substantially Binder-Free Zeolites. U.S. Patent 5,460,796A, 24 October 1995.
82. Pavlov, M.L.; Basimova, R.A. Improvement of Synthesis Methods of Powdery Mordenite Type Zeolite. *J. Oil Gas. Bus.* **2012**, *2*, 459–469.
83. Akolekar, D.; Chaffee, A.; Howe, R.F. The Transformation of Kaolin to Low-Silica X Zeolite. *Zeolites* **1997**, *19*, 359–365. [\[CrossRef\]](#)
84. Rauscher, M.; Selvam, T.; Schwieger, W.; Freude, D. Hydrothermal Transformation of Porous Glass Granules into ZSM-5 Granules. *Microporous Mesoporous Mater.* **2004**, *75*, 195–202. [\[CrossRef\]](#)
85. Scheffler, F.; Schwieger, W.; Freude, D.; Liu, H.; Heyer, W.; Janowski, F. Transformation of Porous Glass Beads into MFI-Type Containing Beads. *Microporous Mesoporous Mater.* **2002**, *55*, 181–191. [\[CrossRef\]](#)
86. Özcan, A.; Kalıpçılar, H. Preparation of Zeolite A Tubes from Amorphous Aluminosilicate Extrudates. *Ind. Eng. Chem. Res.* **2006**, *45*, 4977–4984. [\[CrossRef\]](#)
87. Shimizu, S.; Kiyozumi, Y.; Maeda, K.; Mizukami, F.; Pál-Borbély, G.; Mihályi, R.M.; Beyer, H.K. Transformation of Intercalated Layered Silicates to Zeolites in the Solid State. *Adv. Mater.* **1996**, *8*, 759–762. [\[CrossRef\]](#)
88. Shimizu, S.; Hamada, H. Direct Conversion of Bulk Materials into MFI Zeolites by a Bulk-Material Dissolution Technique. *Adv. Mater.* **2000**, *12*, 1332–1335. [\[CrossRef\]](#)
89. De Luca, P.; Crea, F.; Fonseca, A.; Nagy, J.B. Direct Formation of Self-Bonded Pellets during the Synthesis of Mordenite and ZSM-11 Zeolites from Low Water Content Systems. *Microporous Mesoporous Mater.* **2001**, *42*, 37–48. [\[CrossRef\]](#)
90. Madhusoodana, C.D.; Kameshima, Y.; Yasumori, A.; Okada, K. Preparation of Fiber-Reinforced Binderless Zeolite Disks in Solid State. *J. Mater. Sci. Lett.* **2003**, *22*, 553–556. [\[CrossRef\]](#)
91. Charkhi, A.; Kazemini, M.; Ahmadi, S.J.; Kazemian, H. Fabrication of Granulated NaY Zeolite Nanoparticles Using a New Method and Study the Adsorption Properties. *Powder Technol.* **2012**, *231*, 1–6. [\[CrossRef\]](#)
92. Mañko, M.; Vittenet, J.; Rodriguez, J.; Cot, D.; Mendret, J.; Brosillon, S.; Makowski, W.; Galarneau, A. Synthesis of Binderless Zeolite Aggregates (SOD, LTA, FAU) Beads of 10, 70 µm and 1mm by Direct Pseudomorphic Transformation. *Microporous Mesoporous Mater.* **2013**, *176*, 145–154. [\[CrossRef\]](#)
93. Lei, Q.; Zhao, T.; Li, F.; Wang, Y.F.; Hou, L. Zeolite Beta Monoliths with Hierarchical Porosity by the Transformation of Bimodal Pore Silica Gel. *J. Porous Mater.* **2008**, *15*, 643–646. [\[CrossRef\]](#)
94. Sun, H.; Sun, Z.; Shen, B.; Liu, J.; Li, G.; Wu, D.; Zhang, Y. One-Pot Synthesis of Binderless Zeolite A Spheres via in Situ Hydrothermal Conversion of Silica Gel Precursors. *AIChE J.* **2018**, *64*, 4027–4038. [\[CrossRef\]](#)
95. Zhang, J.; Mao, Y.; Li, J.; Wang, X.; Xie, J.; Zhou, Y.; Wang, J. Ultrahigh Mechanically Stable Hierarchical Mordenite Zeolite Monolith: Direct Binder-/Template-Free Hydrothermal Synthesis. *Chem. Eng. Sci.* **2015**, *138*, 473–481. [\[CrossRef\]](#)
96. Sebakhy, K.O.; Vitale, G.; Pereira-Almao, P. Production of Highly Dispersed Ni within Nickel Silicate Materials with the MFI Structure for the Selective Hydrogenation of Olefins. *Ind. Eng. Chem. Res.* **2019**, *58*, 8597–8611. [\[CrossRef\]](#)

97. Sebakhy, K.O.; Vitale, G.; Pereira-Almao, P. Dispersed Ni-doped Aegirine Nanocatalysts for the Selective Hydrogenation of Olefinic Molecules. *ACS. Appl. Nano Mater.* **2018**, *1*, 6269–6280. [[CrossRef](#)]
98. Asgar Pour, Z.; Koelewijn, R.; El Hariri El Nokab, M.; van der Wel, P.C.A.; Sebakhy, K.O.; Pescarmona, P.P. Binder-free Zeolite Beta Beads with Hierarchical Porosity: Synthesis and Application as Heterogeneous Catalysts for Anisole Acylation. *ChemCatChem* **2022**, *14*, e202200518. [[CrossRef](#)]

Disclaimer/Publisher's Note: The statements, opinions and data contained in all publications are solely those of the individual author(s) and contributor(s) and not of MDPI and/or the editor(s). MDPI and/or the editor(s) disclaim responsibility for any injury to people or property resulting from any ideas, methods, instructions or products referred to in the content.